

## **Bimetallic Nanoplatfom Dedicated to Sonodynamic-Calcium Overload Synergistic Therapy via Self-supplied Hydrogen Peroxide and Relieved Hypoxia**

Wenqian Xu<sup>a†</sup>, Yisheng Zhao<sup>b†</sup>, Chao Zhang<sup>c†</sup>, Mengping Huo<sup>a</sup>, Lei Wang<sup>a</sup>, Xuewu Wu<sup>d</sup>, Yang Zhang<sup>a,\*</sup>, Qiao Li<sup>a,\*</sup>, Yonghao Gai<sup>a,\*</sup>

<sup>a</sup>Department of Ultrasound, Shandong Provincial Hospital Affiliated to Shandong First Medical University, Jinan 250021, P.R. China.

<sup>b</sup>School of Pharmaceutical Sciences, Laboratory of Immunology for Environment and Health, Shandong Analysis and Test Center, Qilu University of Technology (Shandong Academy of Sciences), Jinan 250353, P.R. China.

<sup>c</sup>Department of Pediatrics, Qilu Hospital of Shandong University, Jinan 250012, P.R. China.

<sup>d</sup>Department of Urology, The Second Hospital of Lanzhou University, Gansu Nephro-Urological Clinical Center, Lanzhou 730000, P.R. China.

† Co-first authors, contributed equally to this work.

\* Corresponding authors.

E-mail addresses: ultra\_gaiyonghao@163.com (Y. Gai), 59412061@qq.com (Q. Li),

zhangyang@sdfmu.edu.cn (Y. Zhang).

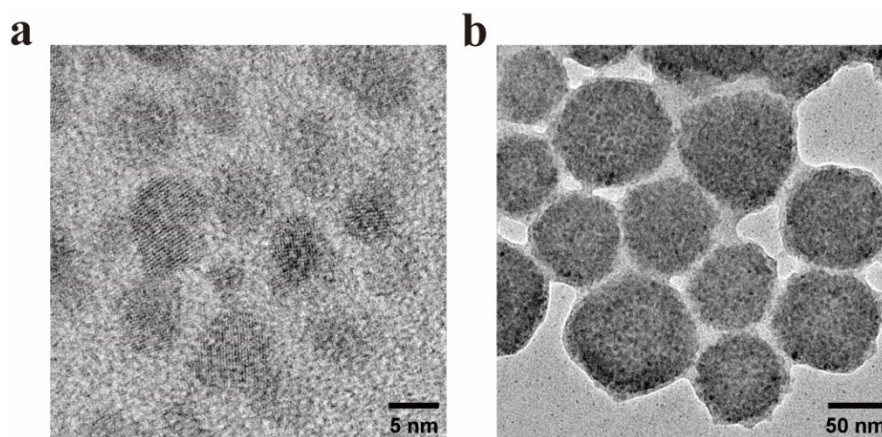


Figure S1. TEM images of a) Fe<sub>3</sub>O<sub>4</sub>-TAPP and b) CaO<sub>2</sub>.

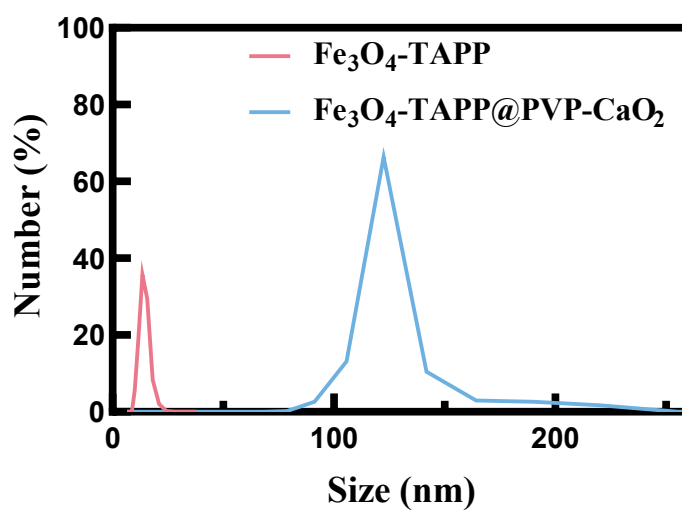


Figure S2. Size distributions of Fe<sub>3</sub>O<sub>4</sub>-TAPP and Fe<sub>3</sub>O<sub>4</sub>-TAPP@PVP-CaO<sub>2</sub> measured by DLS.

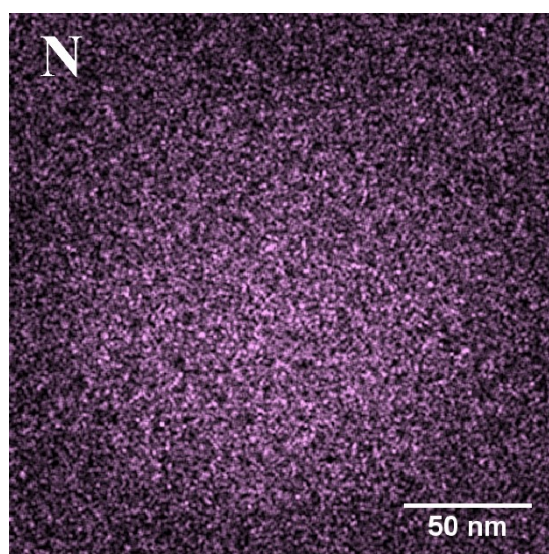


Figure S3. The elemental mapping of N in  $\text{Fe}_3\text{O}_4\text{-TAPP@PVP-CaO}_2$  (scale bar:  $50\mu\text{m}$ ).

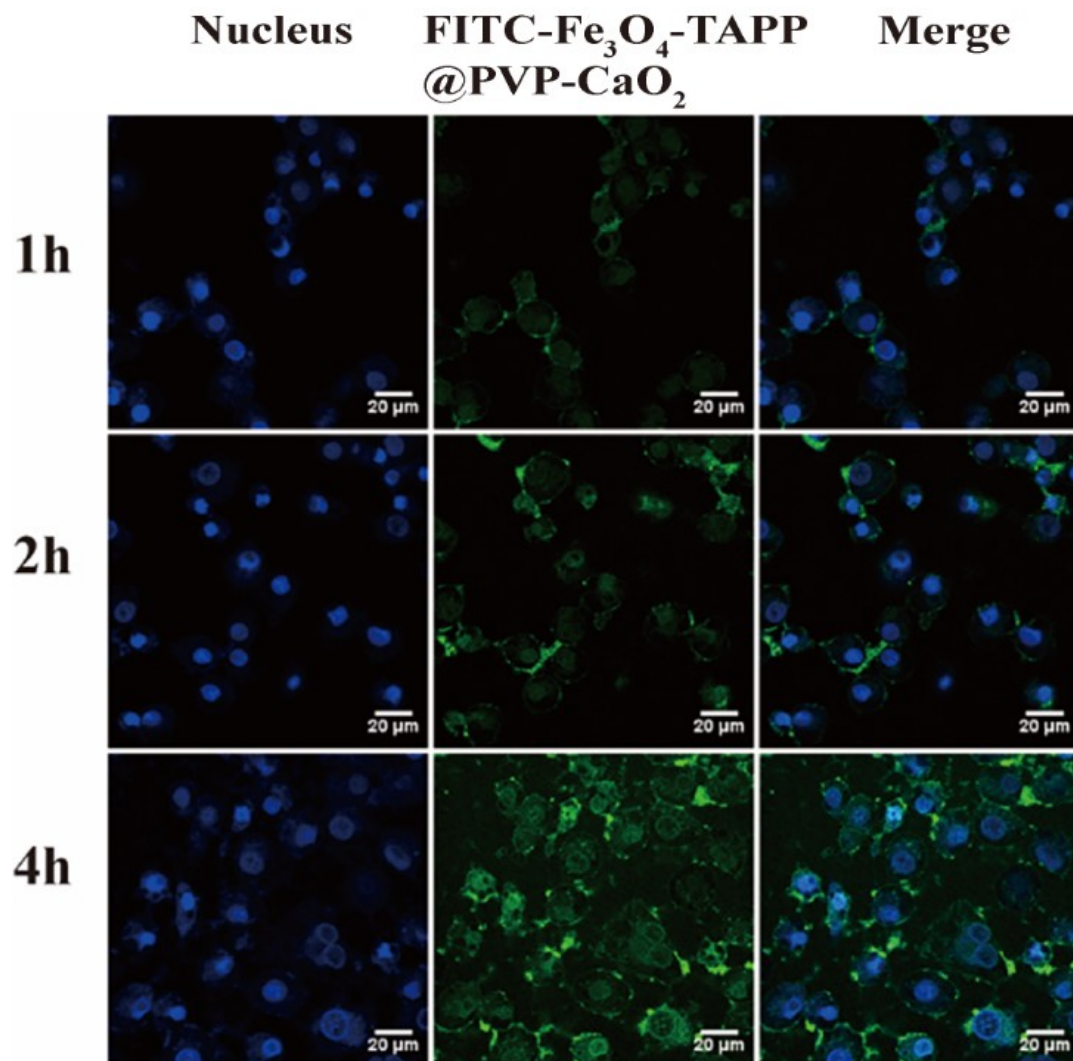


Figure S4. CLSM images of PC-3 cells after treatment with FITC- $\text{Fe}_3\text{O}_4\text{-TAPP@PVP-CaO}_2$  for 1, 2, and 4 h (scale bar:  $20\mu\text{m}$ ).

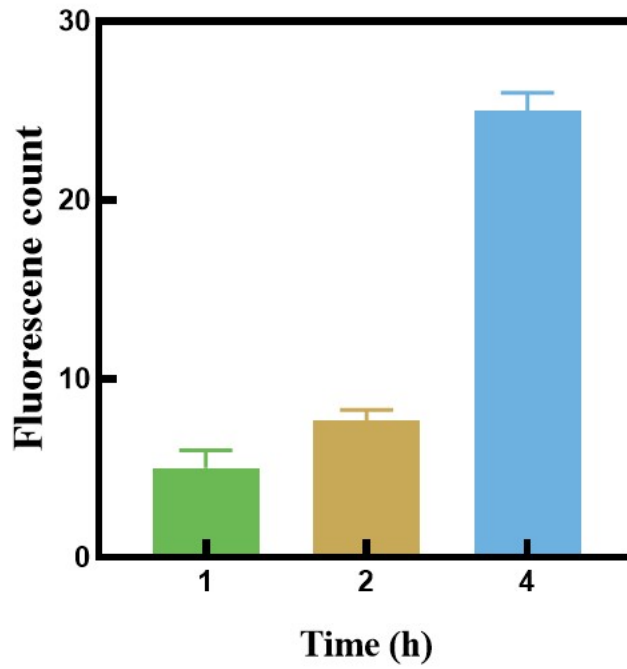


Figure S5. Quantitative cellular uptake of  $\text{Fe}_3\text{O}_4\text{-TAPP@PVP-CaO}_2$  by PC-3 cells counted using Image J. Error bars represent standard deviation of three representative cells.

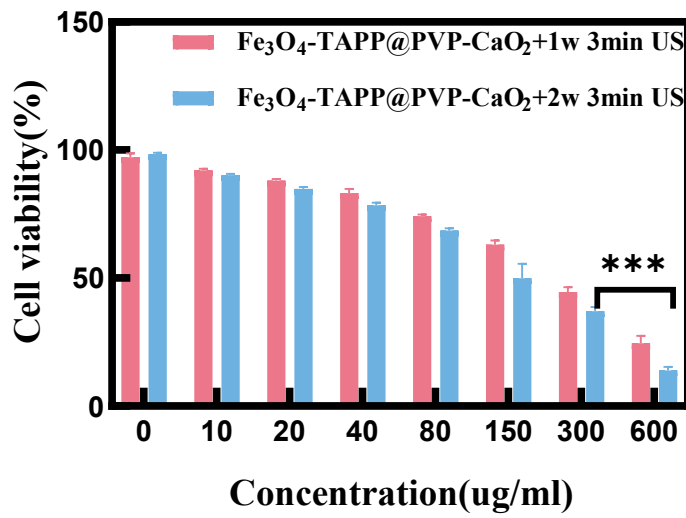


Figure S6. Cell viability of PC-3 cells after co-incubated different concentrations of  $\text{Fe}_3\text{O}_4\text{-TAPP}$  and  $\text{Fe}_3\text{O}_4\text{-TAPP@PVP-CaO}_2$  under US irradiation at different powers.

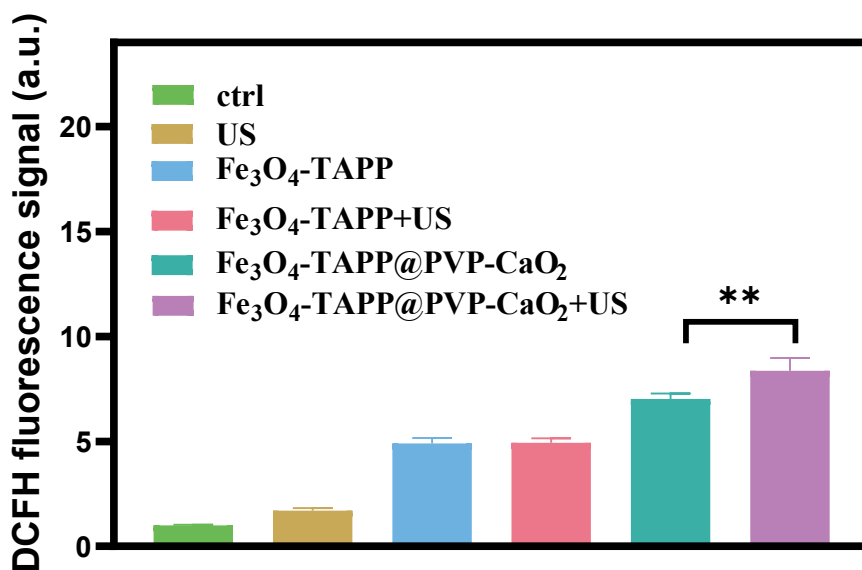


Figure S7. Semiquantitative analysis of ROS-related fluorescence intensity in Figure 2e by Image J software. Data are presented as the mean  $\pm$  SD (n = 3). Significant differences were assessed using t test (\*\*p < 0.01).

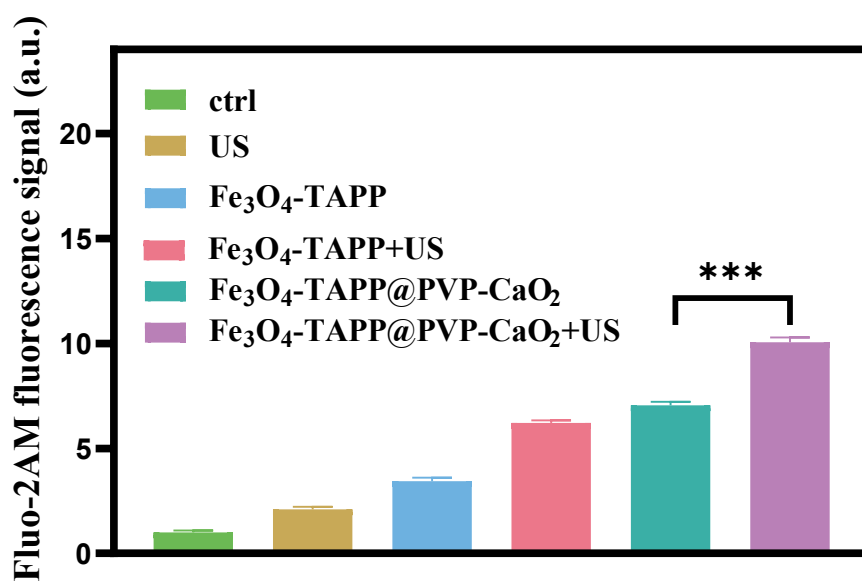


Figure S8. Semiquantitative analysis of Fluo-2AM fluorescence intensity. Data are represented as mean  $\pm$  SD (n = 3; \*\*\*P < 0.001).

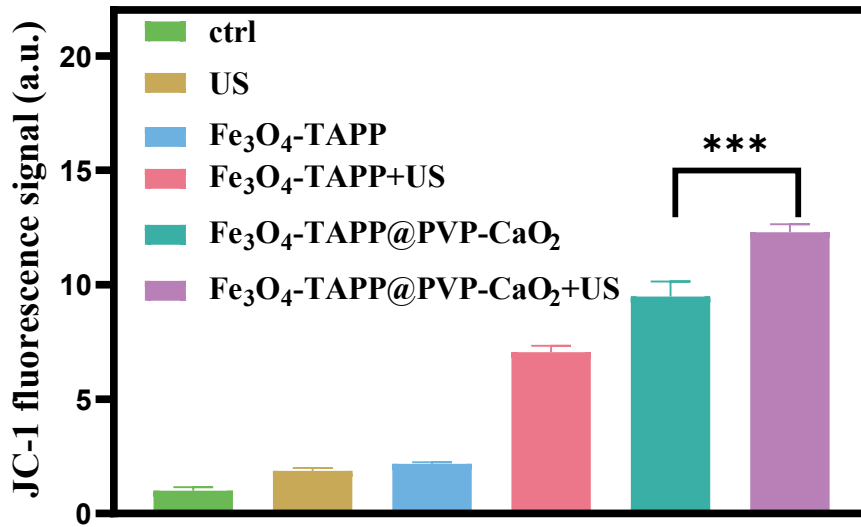


Figure S9. Semiquantitative analysis of JC-1 fluorescence intensity. Data are showed as mean  $\pm$  SD (n = 3; \*\*\*P < 0.001).

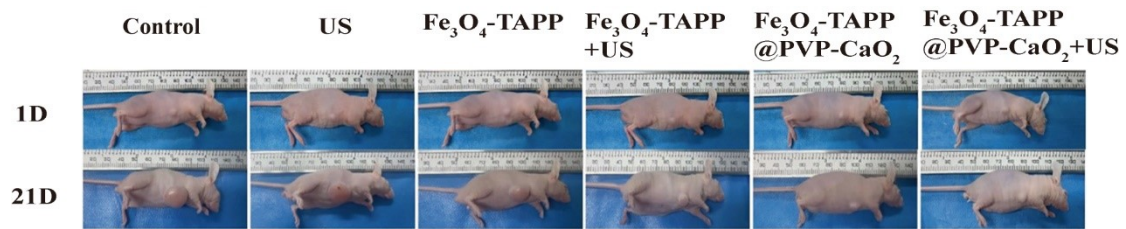


Figure S10. Representative images of mice in the different treatment groups at the indicated time points.

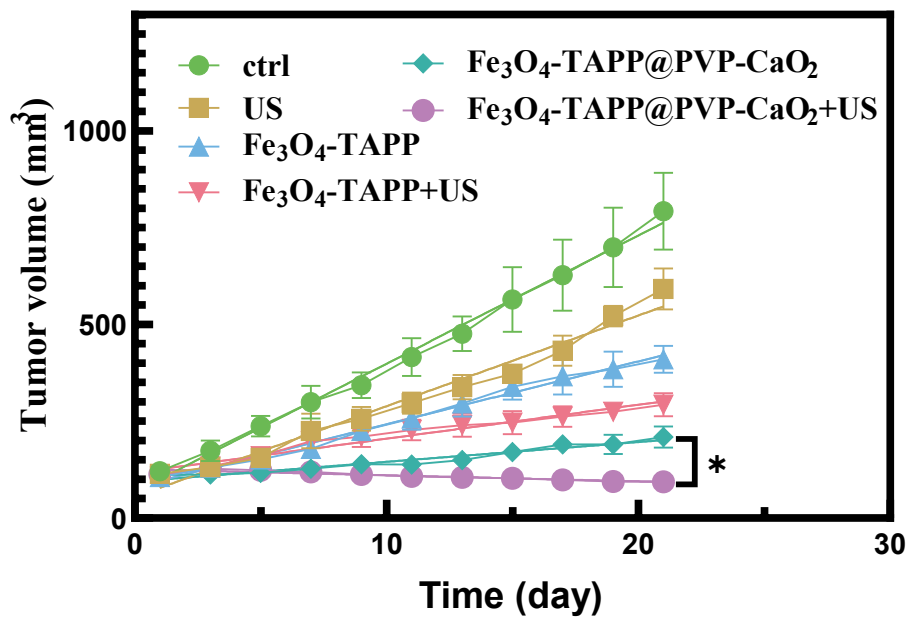


Figure S11. Individual tumor-volume variations of mice after diverse treatments.

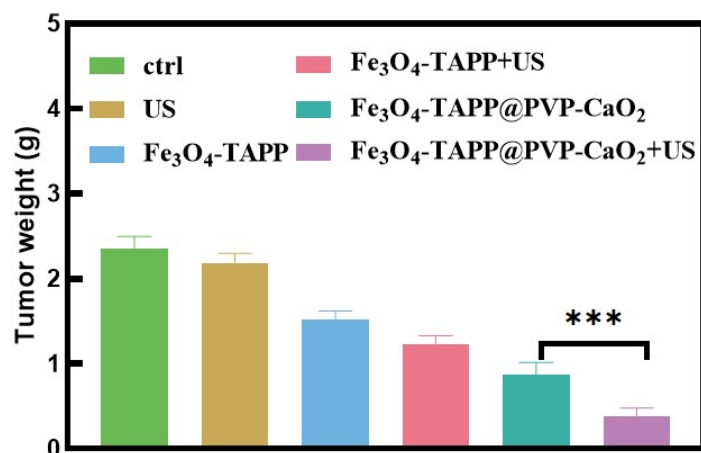


Figure S12. The weight of the excised tumors from the indicated groups.

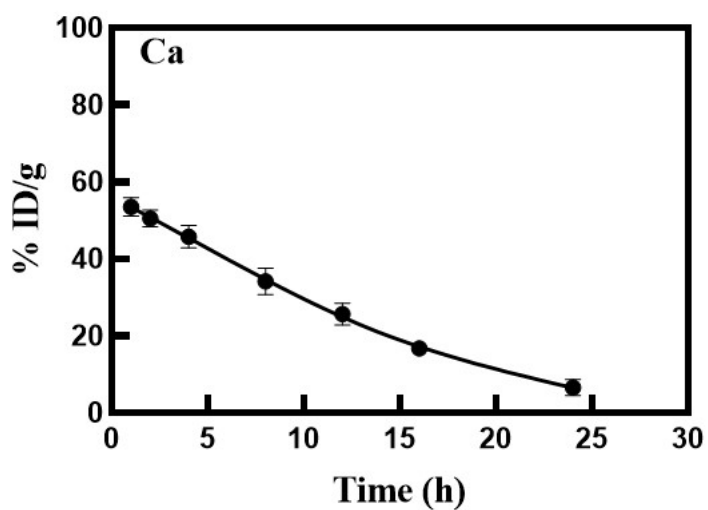


Figure S13. Concentrations of Ca in the blood of mice after the intravenous injection of Fe<sub>3</sub>O<sub>4</sub>-TAPP@PVP-CaO<sub>2</sub> (5 mg/kg).

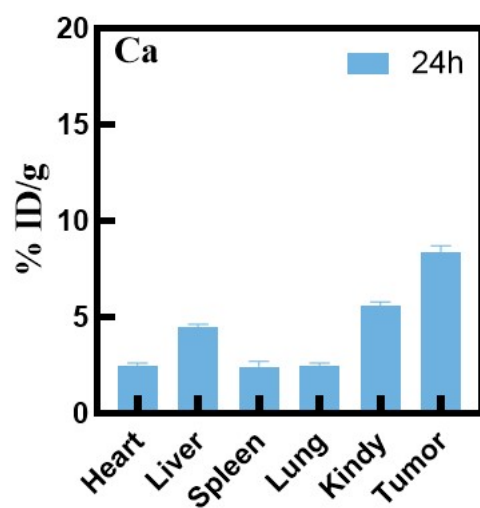


Figure S14. The biodistribution of  $\text{Fe}_3\text{O}_4\text{-TAPP@PVP-CaO}_2$ .

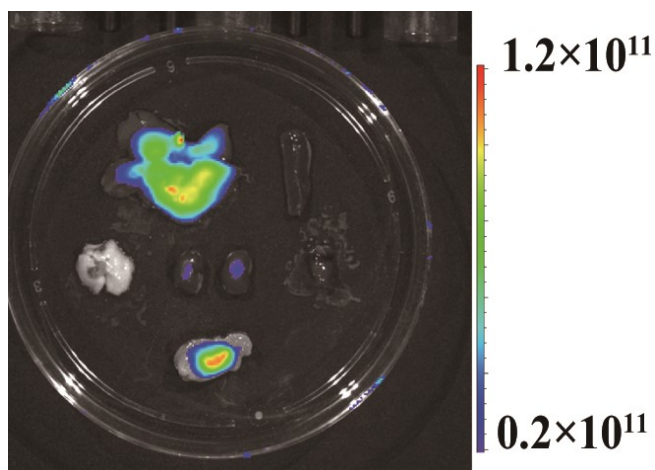


Figure S15. Fluorescence image of organs and tumor tissues.



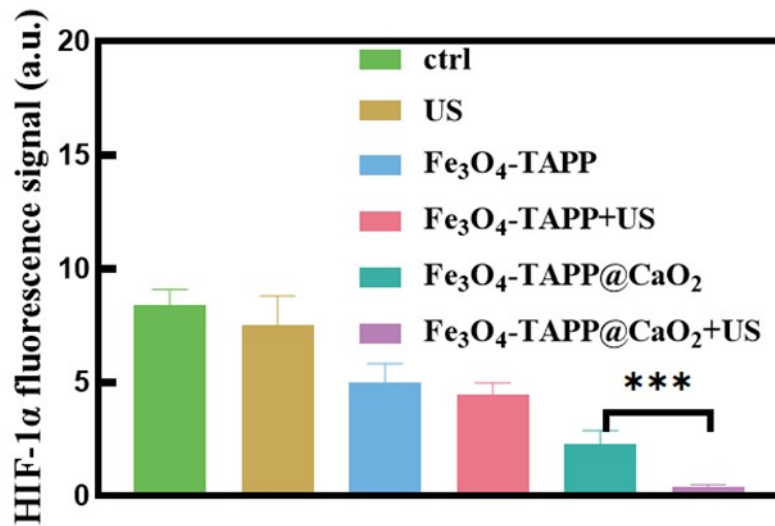


Figure S16. Semiquantitative analysis of HIF-1 $\alpha$  staining of tumor tissues in various treatment groups.

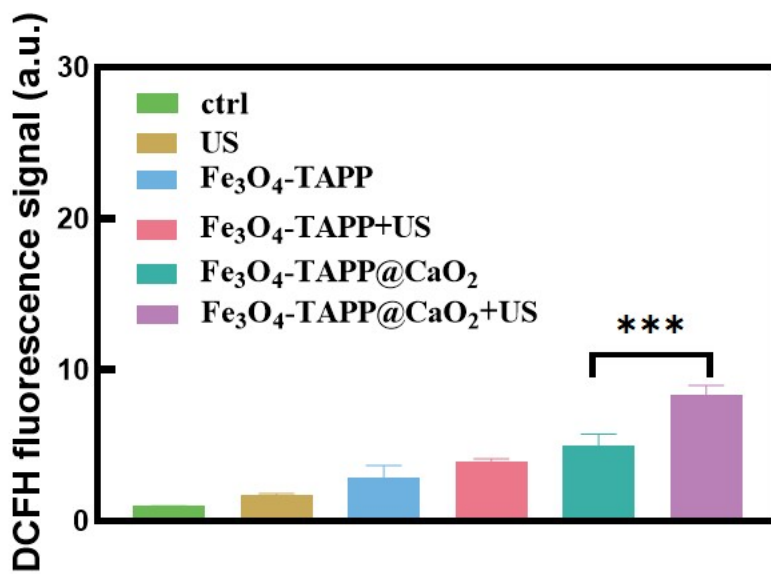


Figure S17. Semiquantitative analysis of DCFH-DA of tumor tissues in various treatment groups.

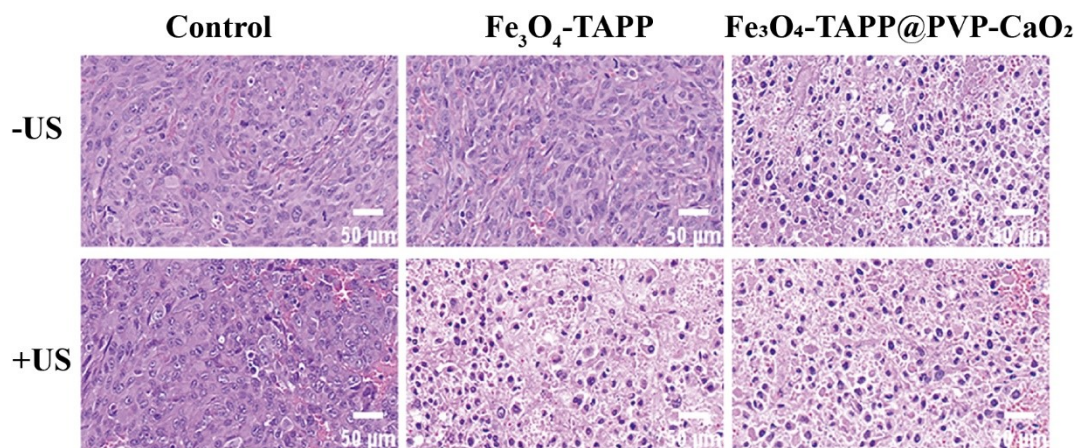


Figure S18. HE of tumor sections harvested at the sixth day in diverse treatment groups. Scale bars are 50 $\mu\text{m}$ .

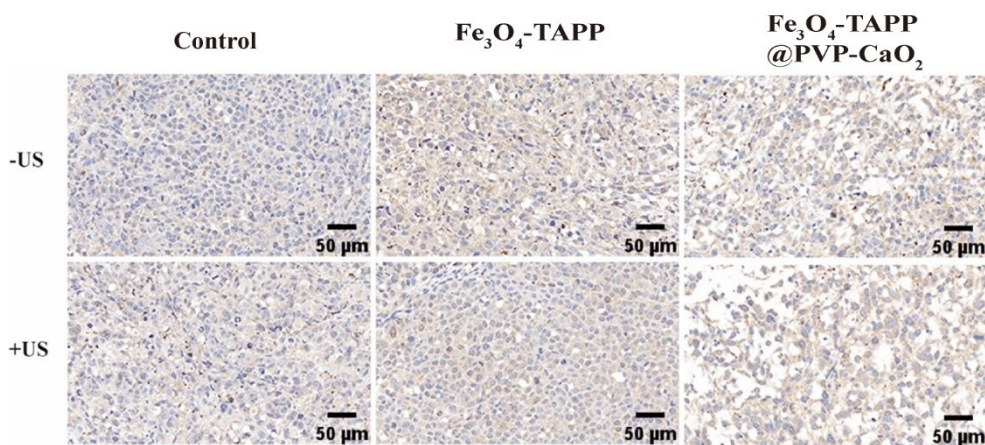


Figure S19. Caspase-3 immunofluorescence staining of tumor sections harvested at the fifth day in diverse treatment groups. Scale bar: 50 $\mu\text{m}$ .

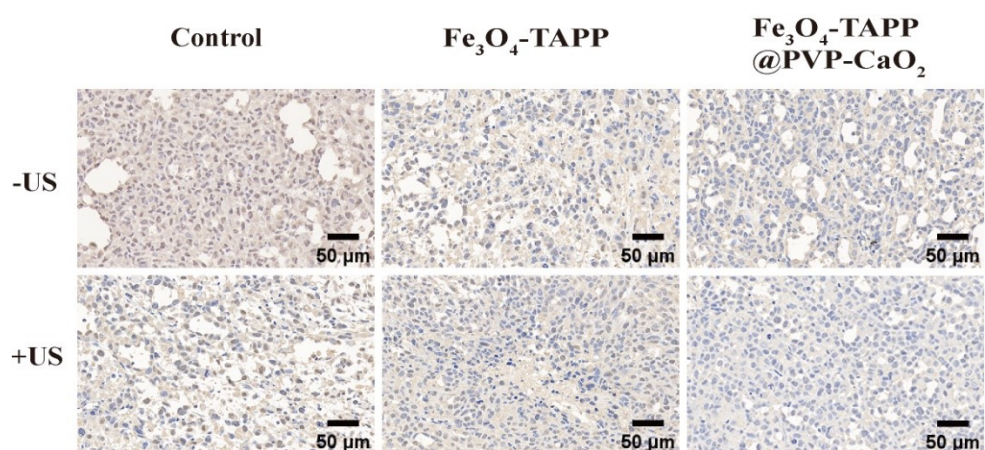


Figure S20. PCNA immunofluorescence staining of tumor sections harvested at the fifth day in diverse treatment groups. Scale bar: 50 $\mu\text{m}$ .

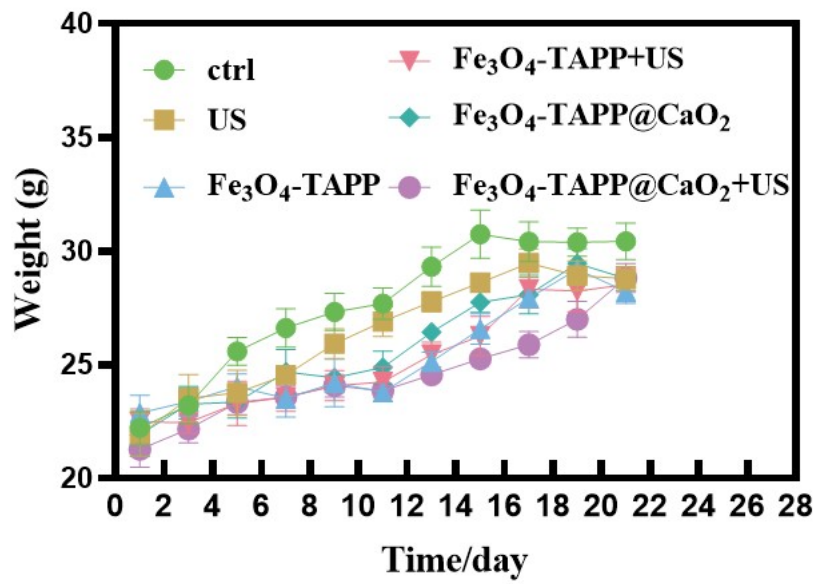


Figure S21. Body weight of different groups of tumor-bearing mice during treatment (n = 5, mean ± SD).

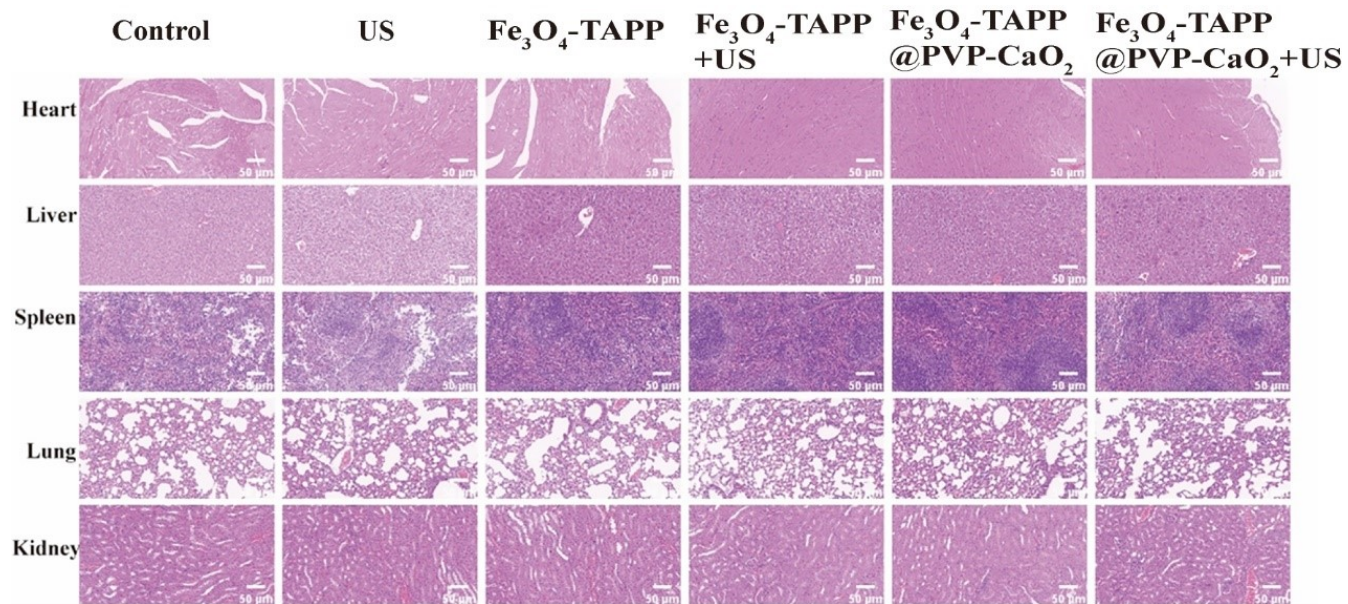


Figure S22. Images of H&E-stained sections of the heart, liver, spleen, lung and kidney from mice in each treatment group.

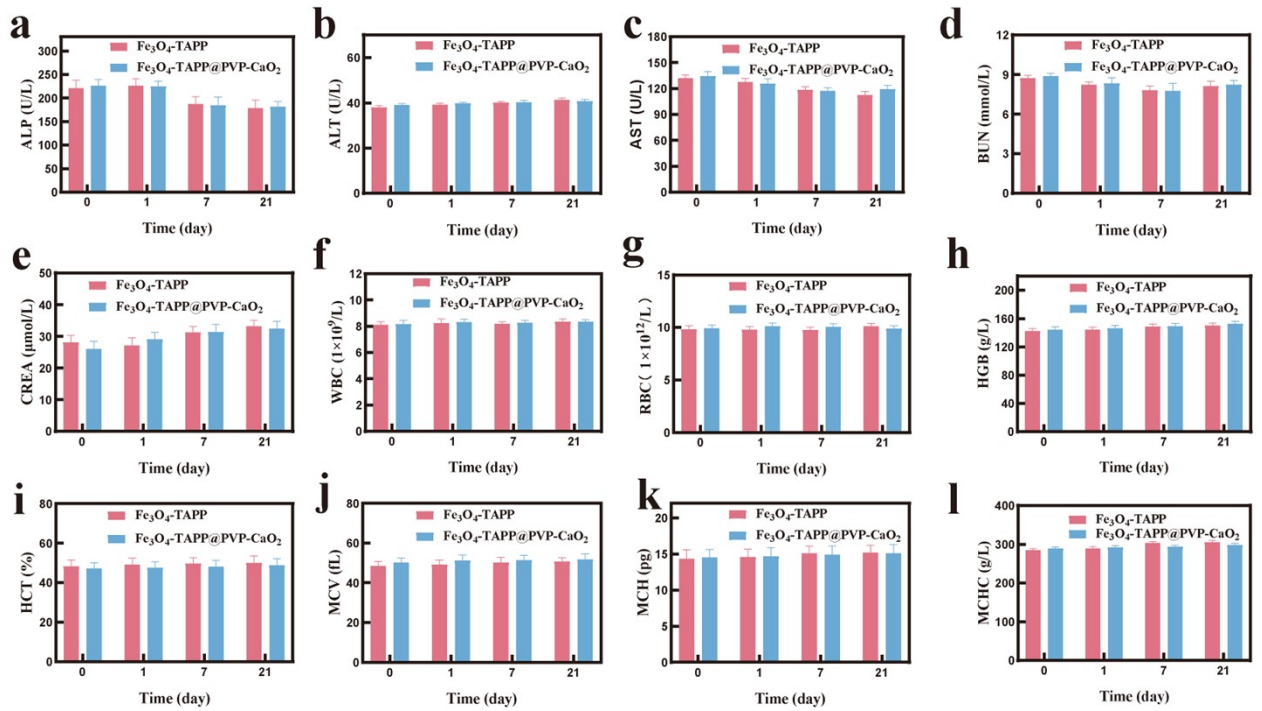


Figure S23. Liver function, renal function and blood panel parameters of BALB/c mice recorded on day 1 and day 21 after intravenous administration of  $\text{Fe}_3\text{O}_4\text{-TAPP}$  and  $\text{Fe}_3\text{O}_4\text{-TAPP@PVP-CaO}_2$  at doses of 5 mg/kg. ALT (A), alanine aminotransferase; AST (B), aspartate aminotransferase; ALP (C), alkaline phosphatase; BUN (D), blood urea nitrogen; CREA (E), creatinine; WBC (F), white blood cells; RBC (G), red blood cells; HGB (H), hemoglobin; HCT (I), hematocrit; MCV (J), mean corpuscular volume; MCH (K), mean corpuscular hemoglobin; MCHC (L), mean corpuscular hemoglobin concentration (n = 5, p > 0.05).